Journal of Physiology (1992), **448**, *pp.* 709–727
With 11 *figures*
Printed in Great Britain

ROLE OF AN INWARDLY RECTIFYING POTASSIUM CURRENT IN RABBIT VENTRICULAR ACTION POTENTIAL

BY Y. SHIMONI, R. B. CLARK AND W. R. GILES*

From the Departments of Medicine and Medical Physiology, The University of Calgary, Calgary, Alberta, Canada T2N 4N1

(*Received 20 May 1991*)

SUMMARY

1. Whole-cell voltage-clamp measurements were made of the time- and voltage-dependent properties of the inwardly rectifying background potassium current I_{K1}, in single myocytes from rabbit ventricle. The main goal of these experiments was to define the role of I_{K1} in the plateau and repolarization phases of the action potential (AP).

2. Action potentials from single ventricular myocytes were used as the command signals for voltage-clamp measurements. In these 'action potential voltage-clamp' experiments, I_{K1} was isolated from other membrane currents by taking the difference between control currents and currents in K^+-free bathing solution. The results show that I_{K1} is small during the plateau, but then rapidly increases during repolarization and declines in early diastole.

3. Evidence of an important functional role for I_{K1} in AP repolarization was obtained by comparing the magnitude of I_{K1} and the rate of change of membrane potential (dV_m/dt) in the same cell during the AP. The time courses of I_{K1} and dV_m/dt during the AP were closely correlated, indicating that I_{K1} was the principal current responsible for final repolarization.

4. Rectangular voltage-clamp steps were used to study time- and voltage-dependent changes in I_{K1} at membrane potentials corresponding to the repolarization phase of the AP. 'Slow' relaxations or tail currents, lasting 100–300 ms, were consistently recorded when the cell was repolarized to potentials in the range −30 to −70 mV, following depolarizations between +10 and −10 mV.

5. The close correlation between the magnitude of the steady-state I_{K1} (in an external K^+ concentration of 5·4 mM), which was outward for membrane potentials in the range −30 to −70 mV, and the magnitude of the tail currents, suggests that they resulted from a slow increase, or reactivation, of I_{K1}.

6. The component of the slow tails due to reactivation of I_{K1} can be separated from a previously described component due to Na^+–Ca^{2+} exchange since the I_{K1} component: (i) does not depend on the presence of the calcium current, I_{Ca}; (ii) can be recorded when internal EGTA (5 mM) suppresses large changes in $[Ca^{2+}]_i$; (iii) does not depend on the Na^+ electrochemical gradient; (iv) is abolished in K^+-free external solution; and (v) is not present in rabbit atrial myocytes, in which I_{K1} is very small.

* To whom all correspondence and reprint requests should be addressed.

MS 9402

7. The time- and voltage-dependent properties of I_{K1} revealed by these tail current experiments suggest that the measured magnitude of I_{K1} will be dependent on the voltage-clamp protocol. Application of a 'conditioning' depolarization preceding a ramp reduces the magnitude of I_{K1} recorded during the ramp. The magnitude of I_{K1} also depends on the rate of change of membrane potential during the ramp; 'faster' ramps produced less outward I_{K1}.

8. These results show that I_{K1} is 'inactivated' during the upstroke and plateau phases of an AP and consequently the amount of I_{K1} available for repolarization is less than the maximal I_{K1} present in the cell. Thus, heart rate-induced changes in I_{K1} may contribute to alterations in the plateau and/or the duration of the action potential, as well as the threshold for firing Ca^{2+}-dependent action potentials, or slow responses.

INTRODUCTION

The existence of a potassium conductance which exhibits inward rectification and plays a functional role in controlling the resting potential and the action potential duration in mammalian heart has been appreciated for more than 30 years (Hutter & Noble, 1960; Noble, 1965, 1984). Whole-cell voltage-clamp measurements and patch-clamp recordings of this current in single mammalian ventricular myocytes have yielded data describing: (i) many of its fundamental kinetic and selectivity properties (Carmeliet, 1982; Sakmann & Trube, 1984*a*, *b*; Kurachi, 1985; for reviews see Rudy, 1988; Adams & Nonner, 1989); (ii) a 'cross-over' phenomenon when external potassium, $[K^+]_o$, is changed (Hille & Schwarz, 1978; DiFrancesco & Noble, 1985; Tseng, Robinson & Hoffman, 1987); and (iii) the marked differences in the density of this current between e.g. atrium and ventricle in guinea-pig (Hume & Uehara, 1985) and rabbit (Giles & Imaizumi, 1988) hearts. In addition, a 'blocking particle' model for the inward rectification, including its negative slope characteristics, has been proposed (Standen & Stanfield, 1978*a*, *b*). The 'blocking particle' has recently been shown to correspond to intracellular magnesium ions inhibiting this K^+ current when it is flowing in the outward direction (Matsuda, Saigusa & Irisawa, 1987; Vandenburg, 1987; Matsuda, 1988, 1991).

In spite of this significant progress, the functional role of the inwardly rectifying potassium current (I_{K1}) during the mammalian cardiac action potential has not been clearly defined (cf. Giles & Imaizumi, 1988; Oliva, Cohen & Pennefather, 1990). One reason for this is that in the heart I_{K1} was originally described as being 'quasi-instantaneous'. Although recent work has demonstrated convincingly that I_{K1} can exhibit time and voltage dependence (Carmeliet, 1982; Kurachi, 1985; Biermans, Vereeke & Carmeliet, 1987), these results have suggested that the time- and voltage-dependent phenomena are detectable only at membrane potentials far hyperpolarized to the normal resting membrane potential (e.g. Harvey & ten Eick, 1988, 1989*a*, *b*).

In the present experiments, we have attempted to identify the time- and voltage-dependent properties of I_{K1} which may be important in modulating repolarization and therefore in controlling the action potential duration in rabbit ventricle. The two experimental approaches which we have used involve (1) voltage-clamping single myocytes with an action potential waveform previously recorded from the same cell,

and (2) application of linear ramp voltage-clamp commands. Our findings indicate that a small, but functionally significant, 'inactivation' of I_{K1} takes place at membrane potentials corresponding to the action potential plateau, and that I_{K1} exhibits time- and voltage-dependent reactivation during repolarization of the action potential, as well as in early diastole. Some of the conditions under which the time- and voltage-dependent changes in I_{K1} during the plateau and repolarization may be important are described and discussed.

METHODS

Solutions and drugs

Standard 'external' HEPES-buffered Tyrode solution contained (mM): NaCl, 140; KCl, 5·4; $CaCl_2$, 1·8; $MgCl_2$, 1; HEPES, 10; glucose, 5·5. The pH was titrated to 7·4 using appropriate amounts of 1·0 M-NaOH. In some experiments, the concentration of KCl was decreased to 2 mM or increased to 10 mM. '0 K^+' solution was made by omitting KCl from standard solution. '0 Na^+' solution was made by replacing NaCl by LiCl. $CdCl_2$ (300 μM), 4-aminopyridine (4-AP; 2 mM), tetrodotoxin (TTX; 25 μM) and ouabain (25 μM) were added to the solutions, as described below. Solutions were gassed with 100% O_2.

The 'internal' (pipette) solution contained (mM); potassium aspartate, 120; KCl, 20; $MgCl_2$, 1; Na_2 ATP, 5; EGTA; 1; HEPES, 10. In some experiments the concentration of EGTA was increased to 5 mM. The pH was titrated to 7·2 with appropriate amounts of 1·0 M-KOH.

Analar grade chemicals (BDH Chemicals Ltd, Poole, UK) were used for making solutions. $CdCl_2$, 4-AP, TTX and ouabain were obtained from Sigma Chemical Co. (St Louis, MO, USA).

Cell dissociation procedure

Adult rabbits (1–2 kg) were killed by cervical dislocation. Ventricular and atrial myocytes were prepared using a dissociation method similar to that described previously by Giles & Imaizumi (1988).

Electrophysiological and data-recording procedures

Myocytes were placed in a recording chamber (volume 200 μl) mounted on the stage of an inverted microscope (Diaphot; Nikon, Tokyo, Japan) and superfused by gravity at about 0·5 ml/min with standard external solution. The experiments were performed at room temperature (21–22 °C), or at 32–33 °C where noted using an electrically controlled heating stage (Toyotomi & Momose, 1989).

Whole-cell patch-clamp recordings (Hamill, Marty, Neher, Sakmann & Sigworth, 1981) were made from ventricular and atrial myocytes using a commercially available amplifier (L/M-EPC 7; List Medical Electronic, Darmstadt, Germany). Patch electrodes were made from borosilicate glass tubing (TW150; WP Instruments, New Haven, CT, USA), and had DC resistances of 2–4 MΩ when filled with 'internal' solution.

A 'local' superfusion system was used to apply test solutions to myocytes within 1–2 s. This consisted of a multi-line pipette system, somewhat similar to that described by Carbone & Lux (1987). Three microbore (0·28 mm inside diameter) polyethylene tubes (PE-10; Clay Adams, Parsipanny, NJ, USA) were cemented with epoxy into a glass capillary tubing with a 1 mm inside diameter, with the ends of the polyethylene tubes protruding about 2–3 mm beyond the end of the glass tube. A patch pipette was pulled from another piece of the same capillary tubing, and the tip of the pipette was broken, then heat-polished under a microforge to produce an opening of 50–100 μm diameter. The tip of the pipette was cut to a length of 5–6 mm and then was cemented over the ends of the polyethylene tubes to form a 'nozzle'. Each of the polyethylene tubes was connected to a 10 ml reservoir via an electrically operated solenoid valve (EXAK-2; Takasago Electric Inc., Nagoya, Japan). The flow rate through each tube (about 50–100 μl/min) was regulated hydrostatically (approx. 20 cmH_2O). The top of the pipette was placed 100–200 μm from the myocyte. One of the tubes contained standard Tyrode solution, and the cell was continuously superfused with this solution between applications of test solutions from the other tubes.

Membrane potential and current were sampled with a 12-bit A/D converter board (DT2801A; Data Translation, Marlborough, MA, USA) at 1 kHz, and stored in a microcomputer using

previously described software (Robinson & Giles, 1986). Membrane currents, voltage-clamp command potentials and current–voltage relationships were plotted using commercial software ('GRAPHER', Golden Software, Golden, CO, USA). Measured membrane potentials were corrected by −10 mV to compensate for the liquid junction potential between the pipette and external solutions.

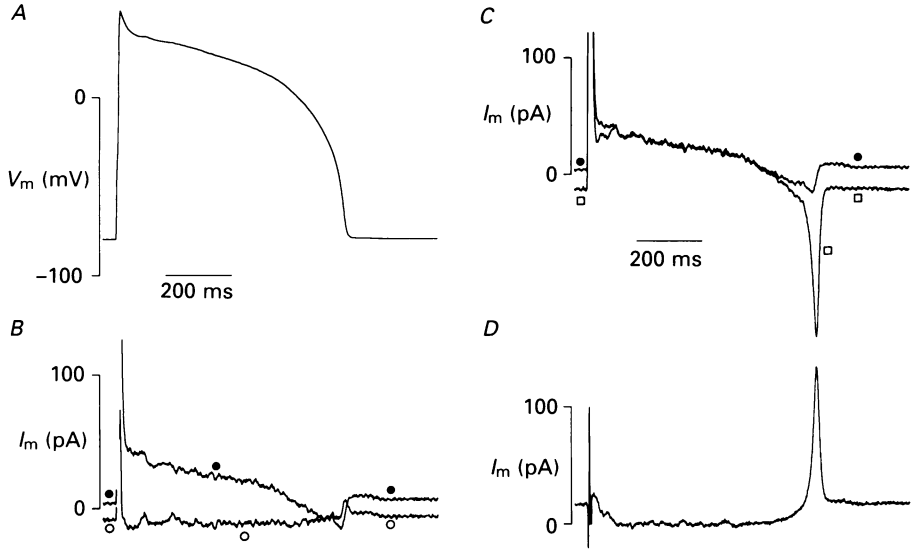

Fig. 1. Illustration of the procedure for measuring I_{K1} using the action potential (AP) voltage-clamp protocol. *A*, the action potential recorded from a rabbit ventricular myocyte was used for the voltage-clamp command signal. *B*, net ionic current (I_m) in response to AP voltage clamp in control conditions (○) was essentially flat, except for a transient during the upstroke of the AP. The solution around the myocyte was changed in less than 2 s to an external solution containing ouabain (25 μM) plus the channel blockers TTX (25 μM), $CdCl_2$ (300 μM) and 4-AP (2 mM). The membrane current during the AP clamp (●) shifted in an outward direction, due to the net effect of reducing inward currents, mainly I_{Ca}. *C*, the effect of switching to a K^+-free external solution. The current after removal of external K^+ (□) reflects all the remaining currents flowing across the cell membrane, minus the potassium background current, I_{K1}. *D*, subtraction of the currents before and after removal of external K^+ gives the net, potassium-sensitive I_{K1} during the AP. Note that the zero on the current scales in this and all subsequent figures refers to zero net membrane current. Temperature was 22 °C.

Action potential and ramp voltage-clamp protocols

The purpose of many of the experiments of this study was to record the time course and magnitude of I_{K1} during a rabbit ventricular action potential (AP). The procedure used in these experiments was to voltage clamp the myocyte with a command signal identical to the AP of the cell (Doerr, Denger, Doerr & Trautwein, 1990). Action potentials were first evoked from a cell in standard HEPES solution ($[K^+]_o$, 5·4 mM) at a rate of 0·33 or 0·25 Hz. The AP (after 10× amplification) was sampled at 16 kHz using a second DT2801A board in another microcomputer. The cell was then voltage clamped at its resting potential (about −80 mV), and repetitively voltage clamped with its AP waveform at the same rate at which the original AP was recorded. The digitally sampled AP was applied to the patch-clamp amplifier using the 12-bit D/A converter on the DT2801A board. The output of the D/A was usually filtered at 0·3–1 kHz before it was applied to the amplifier.

Figure 1 shows an example of the protocols used to isolate I_{K1} during an AP. The AP of an isolated ventricular myocyte bathed in standard external solution is shown in Fig. 1*A*. This AP was recorded and the cell was then voltage clamped with this waveform as described above. The resulting membrane current (marked by ○ in Fig. 1*B*) was essentially flat, except for a large

transient which occurred during the upstroke of the AP. Part of this transient resulted from the voltage-dependent Na^+ current, which could not be controlled under these conditions. The cell was then exposed to solution containing $CdCl_2$, 4-AP, TTX and ouabain. This solution blocked, respectively, the voltage-dependent calcium current I_{Ca}, transient outward K^+ current I_t (Giles & Imaizumi, 1988), voltage-dependent sodium current and the Na^+–K^+ pump current. This resulted in a change in the membrane current during the AP clamp (●, Fig. 1*B*), most notably an outward 'pedestal' of current during the plateau, which probably was due mainly to suppression of I_{Ca} by $CdCl_2$. Finally, the cell was exposed to '0 K^+' solution (also containing $CdCl_2$ etc.). The membrane currents before (●) and after (□) exposure to this solution are compared in Fig. 1*C*. There was little change in the AP clamp current during the plateau, but during the late phase of repolarization there was a large, inward 'spike' of current after exposure to K^+-free solution. The difference in membrane current before and after K^+-free solution was taken as a measure of I_{K1}; this difference is plotted in Fig. 1*D*. Note that the K^+-sensitive current was small (< 20 pA) during most of the AP time course, but was large (> 100 pA) and outward during the terminal phase of repolarization.

Linear ramp voltage-clamp command signals with slopes in the range 0·08–0·8 V/s, generated using the D/A output of the DT2801A board, were used in some experiments. In some cases the ramps were preceded by a rectangular 'conditioning potential' step, as indicated below. Net I_{K1} generated during the ramp potential was obtained by subtracting membrane currents in K^+-containing solution (with $CdCl_2$, etc.) from currents in 0 K^+ solution, as described above. Capacity current will be the same before and after K^+ removal, and it will be eliminated from the difference current.

RESULTS

Action potential voltage-clamp measurements of I_{K1}

The magnitude and time course of K^+-sensitive current during a rabbit ventricular action potential (AP) was determined using the AP voltage-clamp protocols described above. These data showed that the maximal outward currents from single myocytes ranged from 100 to 250 pA ($n = 50$). This outward current increased in magnitude during the final third of the plateau of the AP and exhibited a sharp 'spike' lasting 25–50 ms during the final repolarization phase.

The membrane potential dependence of the K^+-sensitive current was determined by plotting its current–voltage relation during the AP. Figure 2*A* compares the time course of the AP and the K^+-sensitive current from one myocyte. The current–voltage relation for these data, obtained by plotting it *versus* the corresponding membrane potential during AP repolarization, is shown in Fig. 2*B*. The net current at membrane potentials positive to about 0 mV was less than 10 pA, but it gradually increased at more negative potentials, reaching a peak at about −65 mV. This current declined steeply for potentials more negative than −65 mV, and had a reversal potential of about −80 mV. The characteristics of this current–voltage relation, particularly the 'negative slope' between 0 and −65 mV, closely resemble the current–voltage relations for I_{K1} in rabbit ventricle determined previously using conventional rectangular voltage-clamp step protocols (Giles & Imaizumi, 1988). Hence, it was assumed that the K^+-sensitive currents recorded with the protocols described above were due to I_{K1}.

I_{K1} is important for final repolarization in rabbit ventricle

The data shown in Fig. 1*B* imply that the membrane currents blocked by Cd^{2+}, TTX, 4-AP or ouabain make only a very minor contribution to the final repolarization of the rabbit ventricular AP, and hence that I_{K1} is the dominant current controlling final repolarization. Evidence that favours this is shown in Fig. 3, which compares I_{K1} with the rate of change of membrane potential (i.e. dV_m/dt)

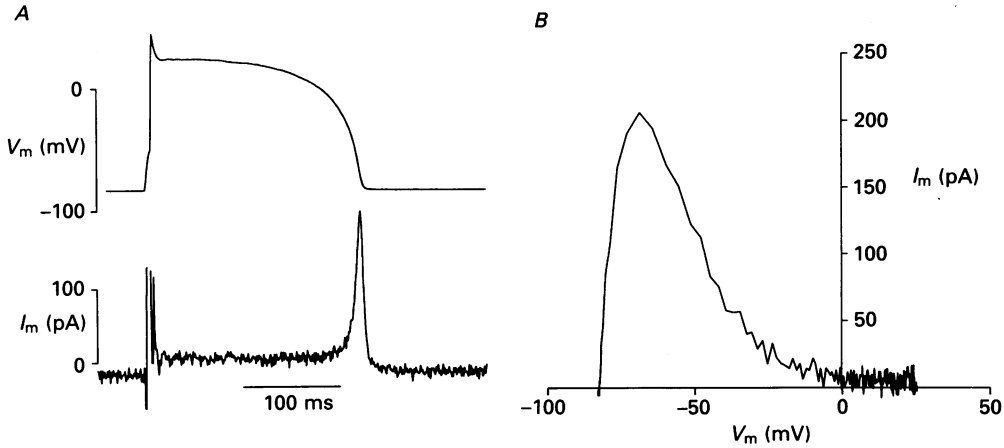

Fig. 2. Current–voltage relationship for I_{K1} during a ventricular AP. *A*, time course of the AP and the corresponding I_{K1} (lower record), obtained using the protocols shown in Fig. 1. *B*, the current–voltage relation for I_{K1} during the AP. Net current (I_m) from *A* is plotted against membrane potential (V_m) during the plateau (starting 5 ms after the peak of the AP) and repolarization phases of the AP. Temperature was 32 °C.

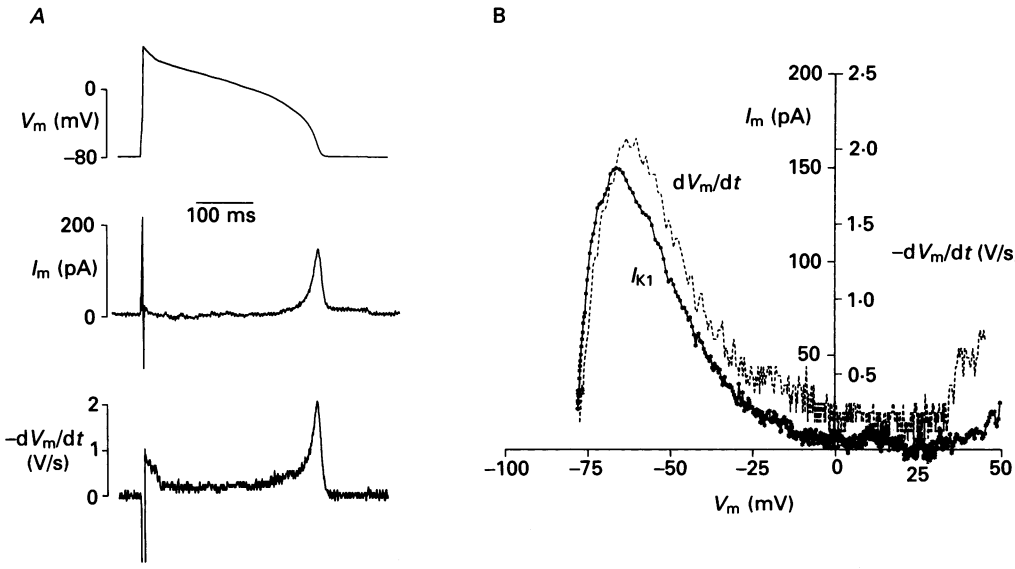

Fig. 3. Comparison of the rate of change of membrane potential (dV_m/dt) and I_{K1} during a ventricular AP. *A*, time course of I_{K1} (middle record) and $-dV_m/dt$ (lower record) during an AP (upper record). *B*, membrane potential dependence of I_{K1} and $-dV_m/dt$ during the plateau and repolarization phases of the AP, from the records in *A*. Note the close correspondence between I_{K1} and dV_m/dt. Temperature was 32 °C.

during an AP. Figure 3*A* shows that the time courses of both I_{K1} and dV_m/dt were closely correlated. Since dV_m/dt is proportional to the net ionic membrane current, this result would be expected if I_{K1} contributed the dominant current change during late AP repolarization. The membrane potential dependence of I_{K1} and dV_m/dt were

very similar, as shown in Fig. 3*B*. The maximum value of dV_m/dt occurred near −60 mV, which was about 5 mV more positive than the potential where maximum I_{K1} was recorded. This may suggest that there is a small contribution from membrane currents other than I_{K1}; nevertheless it is likely that I_{K1} is the most important component of membrane current during the final phase of repolarization.

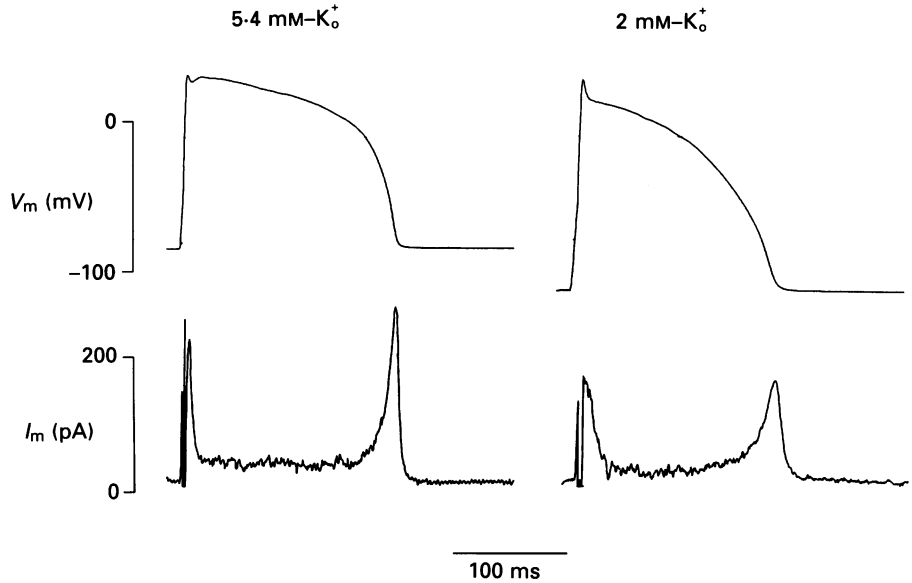

Fig. 4. Effect of external $[K^+]$ on AP configuration and I_{K1}. APs (upper records) and corresponding I_{K1} (lower records) were measured in 2 and 5·4 mM-K_o^+, in the same cell. Note the reduction in amplitude and broadening in time course of I_{K1} when external K^+ was reduced. The external solution used in this experiment to isolate I_{K1} during the AP did not contain 4-AP (cf. Methods). The outward current 'spikes' seen immediately following the initial upstroke of the AP may be transient outward K^+ current, I_t, which was eliminated in most other experiments by 4-AP. Temperature was 22 °C.

Additional data indicating that I_{K1} is the major membrane current controlling final repolarization are shown in Fig. 4. In this cell, when $[K^+]_o$ was reduced from normal values (5·4 mM) to 2 mM, the resting membrane potential hyperpolarized from −83 to −107 mV, the AP duration decreased, and the rate of change of membrane potential during the final phase of repolarization was significantly reduced. Comparison of the net I_{K1} recorded during AP clamp protocols in these two concentrations of external K^+, showed that this decrease in external $[K^+]$ resulted in a reduction in the peak amplitude and a broadening of the time course of I_{K1} underlying the AP. It is likely that the reduced magnitude of I_{K1} was primarily responsible for the reduced rate of final repolarization of the AP in reduced external $[K^+]$.

Time- and voltage-dependent behaviour of I_{K1} in rabbit ventricular myocytes

A number of recent studies have shown that I_{K1} in cardiac myocytes can exhibit both time- and voltage-dependent changes (e.g. Carmeliet, 1982; Matsuda *et al.* 1987; Harvey & Ten Eick, 1989*a*, *b*). The main objective of the remainder of this study was

to determine whether I_{K1} in rabbit ventricular cells exhibited such changes, and whether these changes were important in modulating the AP waveform.

Figures 5 and 6 indicate that time- and voltage-dependent changes in I_{K1} can occur at membrane potentials which correspond to the plateau and repolarization phases

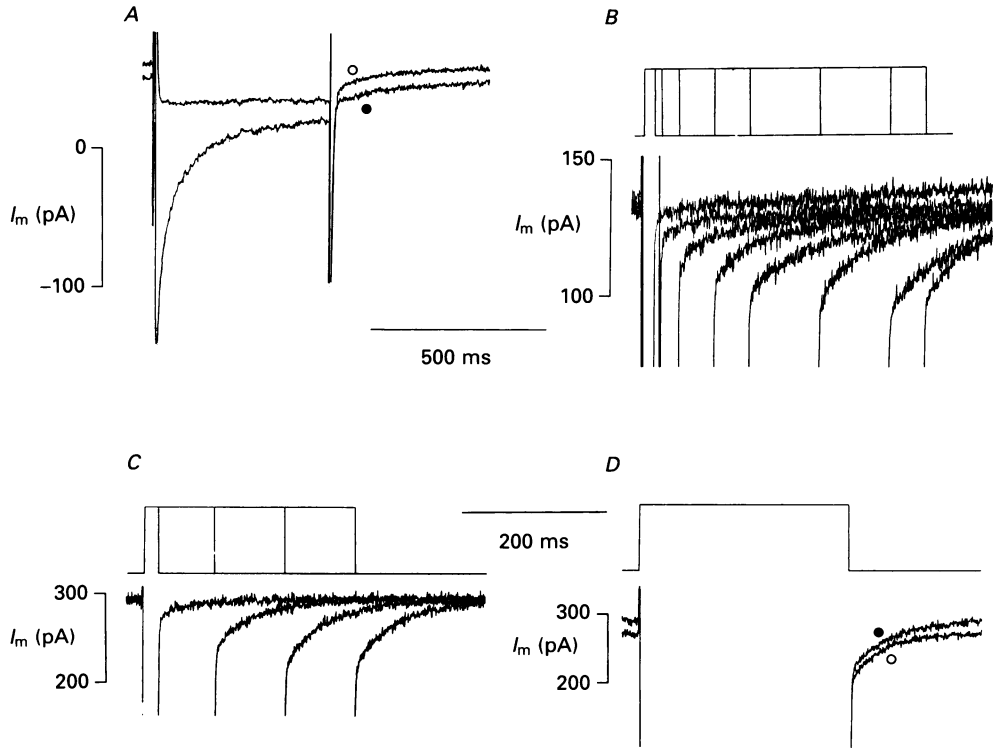

Fig. 5. Properties of inward tail currents in ventricular cells. *A*, this cell (in standard external solution) was depolarized from −50 to 0 mV for 500 ms, then repolarized to −50 mV. Following repolarization, an inward tail current (○) was recorded. This current relaxed back to the holding current level (≈ +60 pA) within about 300 ms. Addition of 0·5 mM-$CdCl_2$ to the external solution completely abolished the inward calcium current during the depolarizing step, but did not significantly alter the tail current (●). *B*, time course of development of inward tail current. This cell was depolarized from −50 to −10 mV for durations ranging from 30 to 800 ms. Note that currents during the depolarization were too large to be seen on this current scale. The amplitude of inward tail currents observed following repolarization were small for short depolarizations, but increased with longer depolarizations and reached a constant amplitude for depolarizations longer than about 500 ms. *C*, tail currents recorded from a myocyte with 5 mM-EGTA in the internal solution (see Methods). The cell was held at −60 mV and stepped to −10 mV for 20, 100, 200 and 300 ms. Note that the increase in tail current amplitude increased with duration of depolarization. *D*, tail currents were not changed by removal of external Na^+. Same cell as in *C*. The cell was held at −60 mV, and depolarized to −10 mV for 300 ms. The inward tail current seen following repolarization (●) was not significantly changed after a fast change to '0 Na^+' solution (○). Note that *A* and *B* have a different time calibration than *C* and *D*. Temperature was 22 °C.

of the AP. In the experiments illustrated in Fig. 5, membrane currents in rabbit ventricular myocytes were recorded in response to rectangular voltage-clamp steps. When myocytes in standard external solution were depolarized to potentials near the

plateau of the AP and then repolarized to potentials in the range −30 to −70 mV, the current slowly relaxed (within 100–300 ms) in an outward direction back to the holding level. Similar 'slow inward' tail currents observed previously in rabbit ventricular myocytes were attributed to the electrogenic activity of the sodium–calcium exchanger (Giles & Shimoni, 1989). However, Fig. 5*A* shows that part of these 'slow inward' tail currents persisted after the calcium current (and hence Ca^{2+} entry) was completely blocked by external application of 0·3 mM-Cd^{2+}. The amplitude of the 'Cd^{2+}-resistant' tail current depended upon the duration of the depolarizing step, as illustrated in Fig. 5*B*. In this example, the cell was voltage clamped at −50 mV, and depolarizations to −10 mV were applied for times between 30 and 800 ms. The amplitude of the inward tail current which was recorded on repolarization to −50 mV increased as the duration of the step to −10 mV was increased over the range 30–500 ms, but then remained relatively constant for longer depolarizations. These results demonstrate that the process giving rise to these tail currents is slow, requiring tens to hundreds of milliseconds to develop. A similar pattern of results was obtained from myocytes ($n = 11$) in which large intracellular calcium transients were prevented by loading the cell with EGTA (5 mM) via the patch pipette solution (Fig. 5*C*). Tail currents also remained following total replacement of Na^+ with Li^+ ($n = 6$; Fig. 5*D*); this treatment would completely inhibit the activity of the sodium–calcium exchanger. It should be noted that most of the experiments in this study were carried out under different conditions than those in which 'slow inward' tail currents were previously studied (Giles & Shimoni, 1989), the most important difference being that at least 1 mM-EGTA was included in the internal solution (see Methods). The results shown in Fig. 5 strongly suggest that processes other than the sodium–calcium exchanger are responsible for generating a portion of the 'slow inward' tail currents in rabbit ventricular cells.

It is not clear from the data shown in Fig. 5 whether the tail currents result from the decay of an inward membrane current, or conversely whether they result from an *increasing* outward current. The results shown in Fig. 6 provide evidence that the tails result from an increase in an outward current, namely I_{K1}. The myocyte was voltage clamped at different holding potentials between −40 to −70 mV, depolarized to −10 mV for 500 ms, and then returned to the holding potential. The magnitudes of I_{K1} and the tail currents at each membrane potential were measured as shown by the sample current record in the inset to Fig. 6*A* (see also figure legend). Note that the membrane potential dependence of I_{K1} and the tail current were very similar; both peaked near −60 mV and both had a negative slope region for more positive membrane potentials. Figure 6*B* shows that I_{K1} and the tail currents were simultaneously abolished by exposing myocytes to either Ba^{2+} (0·5 mM) or '0 K^+' solution, as expected for current changes due to I_{K1}.

Figure 7 shows that the time course of the tail current was quite well described by a single exponential function, the time constant of which was strongly dependent on membrane potential. In Fig. 7*A* examples of single exponential functions fitted to tail currents generated by a two-step voltage-clamp protocol in one myocyte are shown. The rate of relaxation of the tail current became more rapid as the membrane potential during the second voltage step became more negative. In addition, the magnitude of the tail current, compared with the magnitude of the 'steady-state' current at the end of the voltage step, became larger as the membrane potential was

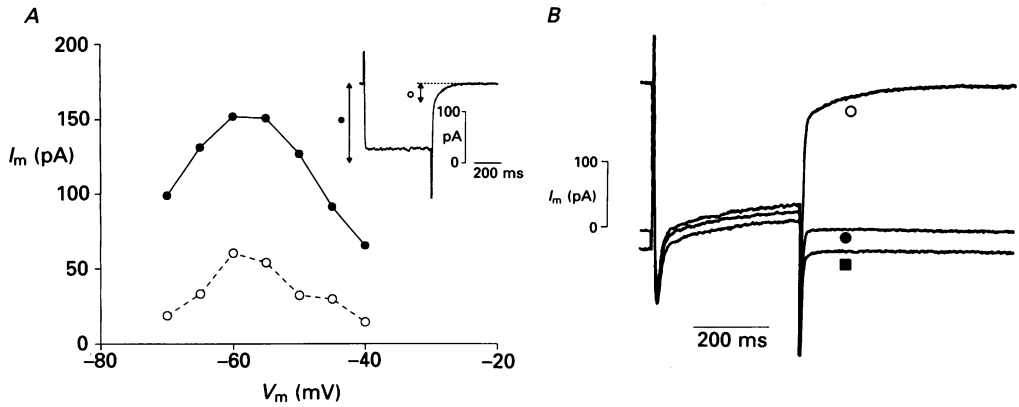

Fig. 6. *A*, correlation between the magnitude of I_{K1} and inward tail current. The cell was depolarized to −10 mV for 500 ms from different holding potentials in the range from −40 to −70 mV. The inset shows the net current (i.e. difference between currents in presence and absence of K_o^+) in response to the step from a holding potential of −50 mV. The magnitude of the 'steady-state' I_{K1} (●) was measured with respect to zero-current level as shown. Inward tail current amplitude (○) was measured at 2 ms after the end of the depolarizing step. I_{K1} and tail current amplitudes were plotted as a function of holding potential. *B*, tail currents (○) in a ventricular cell were abolished by 0·3 mM-$BaCl_2$ in the external solution (●) or by removal of external K^+ (■). Note also the large (≈ 240 pA) inward shift in holding current in Ba^{2+} or in the absence of K_o^+, reflecting abolition of I_{K1}. Tail currents were generated following a 400 ms step to −10 mV, from a holding potential of −55 mV. Temperature was 22 °C.

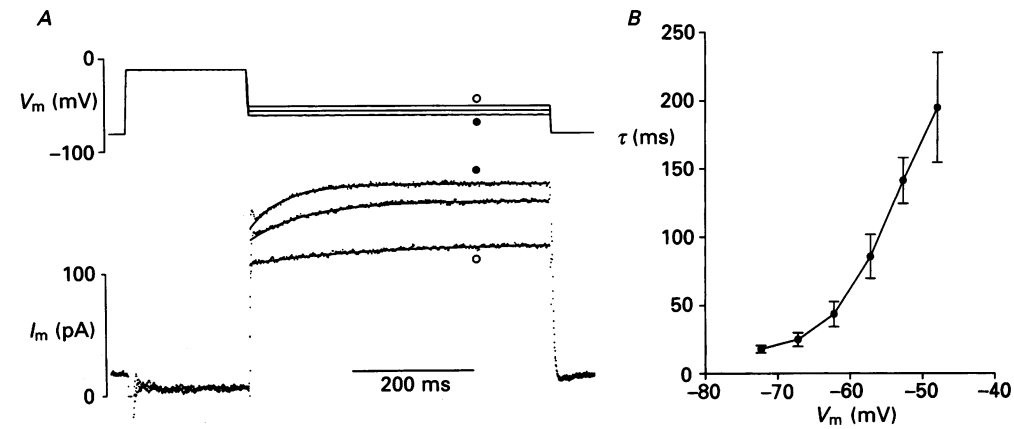

Fig. 7. Membrane potential dependence of tail current time course. *A*, membrane current elicited in a ventricular myocyte by a two-step voltage-clamp protocol (upper traces); currents for three different 'tail' potentials (−51, −56 and −61 mV) are superimposed (lower traces). Leakage currents were removed by subtracting currents after exposure of the myocyte to '0 K^+' solution. Note that the tail current relaxed most rapidly at the most negative membrane potential, −61 mV (●), and slowest at the most positive, −51 mV (○). Single exponential functions (continuous lines) were fitted to the tail currents, with time constants of 56 ms at −61 mV, 93 ms at −56 mV and 192 ms at −51 mV. *B*, plot of mean (±S.E.M.) tail current time constant (τ, from single exponential fits) against membrane potential. Data were pooled from five different myocytes (except at −72 mV, where $n = 4$). Temperature was 22 °C.

made more negative. Figure 7*B* shows the membrane potential dependence of the time constant for these tail currents, including data pooled from five different myocytes. The time constant changed by nearly a factor of ten over the membrane potential range −72 to −48 mV. It was difficult to measure tail currents at

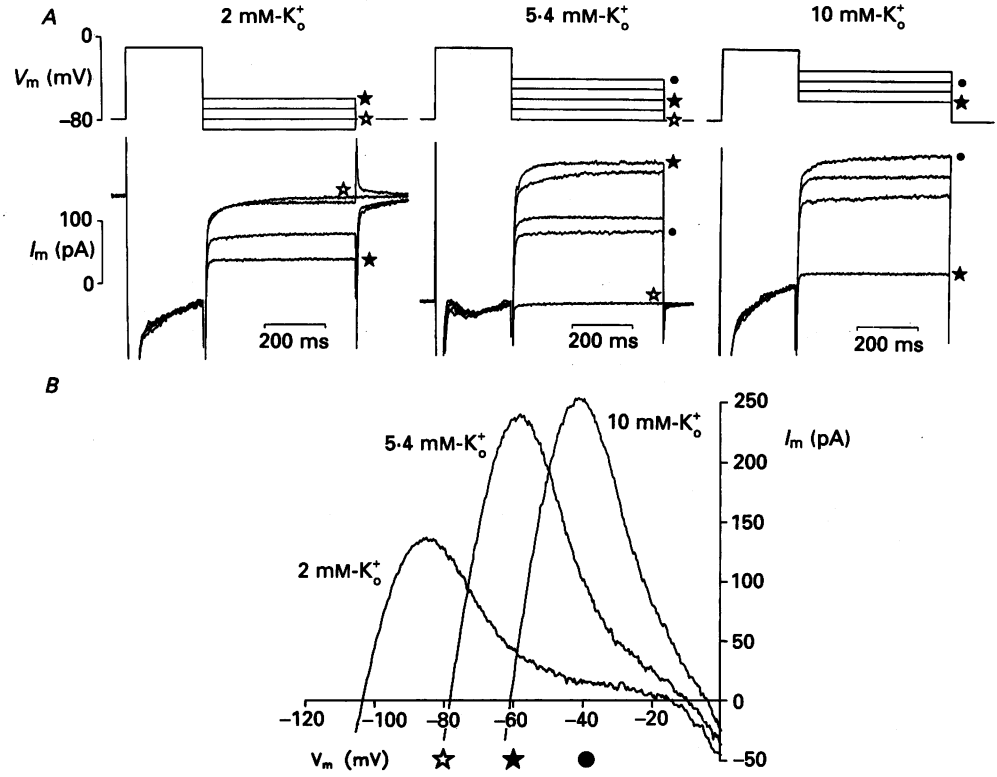

Fig. 8. Correlation between the magnitude of inward tail currents and I_{K1} in different external [K^+]. *A*, families of membrane currents produced by double-pulse voltage-clamp protocols are shown for 2, 5·4 and 10 mM-K_o^+. Tail currents were produced on repolarization from the depolarizing step to a series of different membrane potentials. The symbols indicate potentials of −40 (●), −60 (★) and −80 (☆) mV. The corresponding currents for these potentials in each family are indicated with the same symbols. *B*, current–voltage relations for I_{K1} in 2, 5·4 and 10 mM-K_o^+, generated using a linear potential ramp voltage-clamp protocol (+20 to −110 mV in 1 s, from a holding potential of −80 mV). In this experiment the external solution did not contain the channel blockers of Cd^{2+} and TTX; this accounts for the inward currents between 0 and −20 mV. However, this had no significant effect on the magnitude of I_{K1} in the range of membrane potentials of interest in this experiment, i.e. −40 to −80 mV. Note that the inward tail currents were largest at potentials where I_{K1} was also largest; conversely, small tail currents were recorded at potentials where I_{K1} was also small. Temperature was 22 °C.

membrane potentials more positive than this because of the large time constant, and also because the magnitude of the tail became very small.

Figure 8 provides more evidence that the tail current resulted from time- and voltage-dependent changes in I_{K1}. In this experiment, the membrane potential dependence of the tails was compared with that of I_{K1} in three different external

concentrations of K^+. Figure 8*A* shows families of membrane currents produced by a series of rectangular voltage-clamp steps in 2, 5·4 and 10 mM $[K^+]_o$. In each case, the myocyte was voltage clamped at −80 mV, stepped to −10 mV for 250 ms, and then repolarized to a series of different potentials. The current–voltage relation for I_{K1} at each external $[K^+]$ was generated using a voltage ramp which changed from +20 to −110 mV within 1 s, from a holding potential of −80 mV (Fig. 8*B*). These current–voltage relations showed the 'cross-over' in different $[K^+]_o$ which is characteristic of I_{K1}. The reversal potentials shifted by about 43 mV for the 5-fold change in $[K^+]_o$ for 2 to 10 mM, essentially identical to the 40 mV shift expected for a purely K^+-selective conductance. Comparison of the current–voltage relation for I_{K1}, and the magnitude of tail currents at different membrane potentials, showed that for each $[K^+]_o$, the magnitude of the tail current was largest at membrane potentials where I_{K1} was also largest. For example, tail currents measured at −60 mV (indicated by ★ in the records in Fig. 8*A*) were large in 5·4 mM-K_o^+, but were negligible in 2 and 10 mM-K_o^+. Similarly, the magnitude of I_{K1} in 5·4 mM-K_o^+ was nearly maximal at −60 mV (Fig. 8*B*), whereas the current was relatively small (< 20 %) at the same membrane potential in 2 and 10 mM-K_o^+. On the other hand, the tail current in 5·4 mM-K_o^+ was undetectable at −80 mV (indicated by ☆), which was close to the reversal potential of I_{K1}, but in 2 mM-K_o^+ a large tail current was produced at −80 mV, a potential at which I_{K1} was nearly maximal. A similar shift in the voltage dependence of the tail currents to more negative membrane potentials after a reduction in $[K^+]_o$ was observed in each of twelve different myocytes.

Rabbit atrial cells lack I_{K1} tail currents

Experiments with rabbit atrial myocytes yielded additional data supporting the suggestion that the tail currents in rabbit ventricular myocytes resulted from time-dependent relaxations of I_{K1}. Rabbit atrial cells have only a very small outward I_{K1} (Giles & Imaizumi, 1988) and Fig. 9 shows that 'slow inward' tail currents were not recorded from these cells in conditions where increases in intracellular $[Ca^{2+}]$ were prevented. The left-hand records in Fig. 9 show superimposed currents from an atrial cell before and after addition of Cd^{2+} to the external solution. In this experiment, the patch pipette solution did *not* contain EGTA. The cell was voltage clamped at −50 mV, stepped to +10 mV, then repolarized to −50 mV. In control conditions (○), the step to +10 mV produced a large, rapidly activating inward current, which was followed by a 'slow inward' tail current on repolarization to −50 mV. This tail current has been attributed to activity of the sodium–calcium exchanger (Giles & Shimoni, 1989; Earm, Ho & So, 1990). Following application of 0·3 mM-$CdCl_2$ (●), a transient outward current became apparent during the depolarizing step; this was unmasked by the block of the inward calcium current. In addition, the tail current was completely abolished. This pattern of results in atrial cells contrasts with that in ventricular myocytes, in which large tail currents were consistently observed even after block of I_{Ca}. The right-hand records in Fig. 9 show currents recorded from an atrial cell when the pipette solution contained 5 mM-EGTA. Calcium currents were not blocked, but no tail currents were seen following the depolarizing step. In addition, removal of external K^+ had only a very small effect on the membrane currents, unlike the large changes seen in ventricular myocytes (Fig. 5*B*).

Effect of voltage-clamp protocol on measured I_{K1}

The results in Figs 5–8 show that depolarization of the cell membrane to potentials corresponding to those during the AP plateau can partially 'inactivate' the outward component of I_{K1}, so that following repolarization to more negative potentials, the

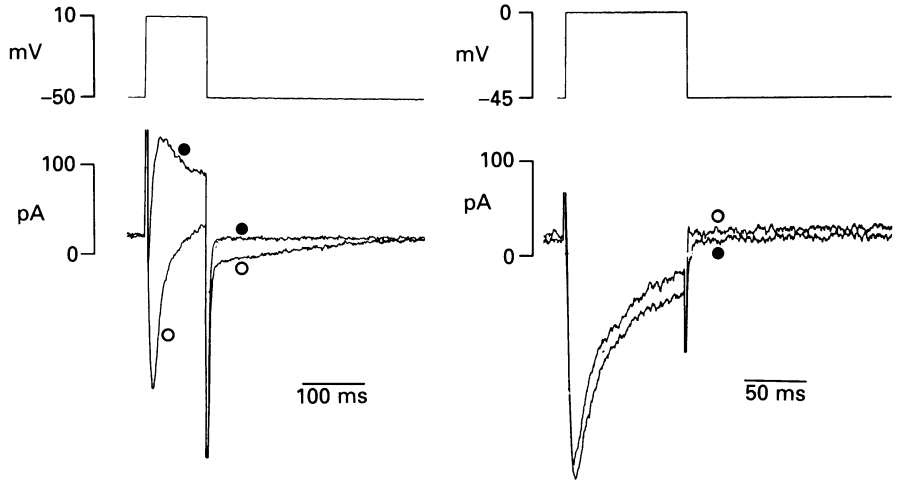

Fig. 9. Absence of inward tail currents in rabbit atrial myocytes. Left, currents in response to a 100 ms depolarization, from −50 to +10 mV, in standard external solution (○), and following addition of 0·4 mM-$CdCl_2$ (●) to the external solution. In this experiment, the internal (pipette) solution did *not* contain EGTA. A slow inward tail current (○) was apparent following the end of the depolarizing step. This tail current was completely abolished after Cd^{2+} (●). Note that a transient outward current was revealed after Cd^{2+} blocked the inward calcium current during the depolarization. Right, an atrial myocyte was voltage clamped with a pipette containing 5 mM-EGTA in the internal solution. Note that there was no inward tail current after the depolarizing step (from −45 to 0 mV) in control solution (○), nor was there any change after switching to '0 K^+' external solution (●), aside from a small (< 10 pA) inward shift in holding current. Temperature was 22 °C.

outward current increases slowly (within 100–300 ms) to its steady-state amplitude at that potential. This effect can decrease the outward I_{K1} by as much as 20–30% of its steady-state amplitude (e.g. Fig. 6*A*). It follows that the measured I_{K1} current–voltage relation will depend on the voltage-clamp protocol which is used to obtain it. Hence, it is probable that the magnitude of I_{K1} recorded during an AP voltage-clamp protocol will be influenced by the waveform of the AP. For example, Fig. 10*A* compares the I_{K1} current–voltage relation in one cell determined using an AP voltage clamp with that obtained from a linear potential ramp, which went from plateau potentials (+20 mV) to more negative potentials (−90 mV) in 500 ms. The time dependences of I_{K1} during the AP and ramp protocols are compared in Fig. 10*A*; note that the peak amplitude of I_{K1} was significantly larger during the ramp protocol than it was during the AP clamp. This is clearly shown in the superimposed current–voltage relations (Fig. 10*B*). I_{K1} from both AP and ramp protocols had their peak magnitudes near −65 mV, but the peak magnitude of I_{K1} during the AP

protocol was about 25% less than that during the voltage ramp. Qualitatively similar results were seen in twenty-nine different myocytes. This result implies that the membrane depolarization which occurred during the plateau of the AP produced more 'inactivation' of I_{K1} than did this ramp protocol.

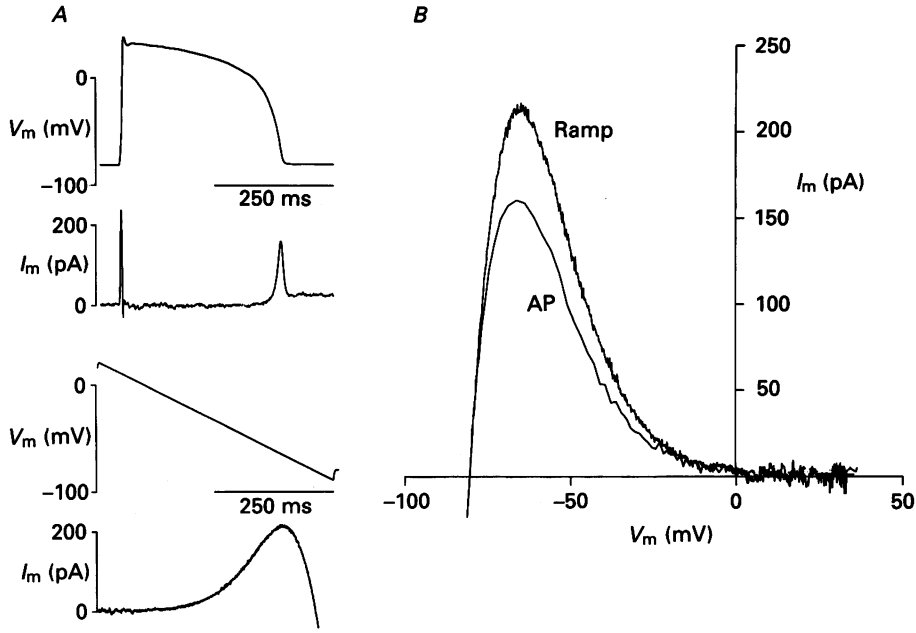

Fig. 10. Comparison of I_{K1} measured in the same myocyte using AP and linear potential ramp voltage-clamp protocols. *A*, the upper pair of records shows the AP and corresponding I_{K1}, while the lower pair of records shows the potential ramp (from +20 to −90 mV, in 500 ms) and corresponding I_{K1}. Holding potential for the ramp protocol was −80 mV. *B*, superimposed current–voltage relations for I_{K1} from the AP and ramp voltage-clamp protocols shown in *A*. Temperature was 32 °C.

The results shown in Fig. 5 suggested that the amount of 'inactivation' of I_{K1} produced by membrane depolarization was dependent on its duration. This was confirmed by the data shown in Fig. 11*A*, where a potential ramp was preceded by a 'conditioning' depolarization of different durations. The I_{K1} current–voltage relations demonstrate that a long (i.e. 1 s) 'conditioning' depolarization produced greater 'inactivation' of I_{K1} than did a short (10 ms) depolarization. A very similar effect was observed in twenty-five different cells. The rate of change of membrane potential was also an important determinant of the magnitude of I_{K1} measured using a ramp. Figure 11*B* compares the I_{K1} current–voltage relations for potential ramps with different rates of change of potential, i.e. −0·4 and −0·08 V/s. Note that the magnitude of I_{K1} was larger during the 'slow', as compared with the 'fast', ramp. A difference in the magnitude of I_{K1} was also observed when ramps were applied in different directions over the same range of membrane potentials (data not shown). Ramps from negative to positive potentials consistently (n = 23) gave more outward I_{K1} than identical ramps from positive to negative potentials.

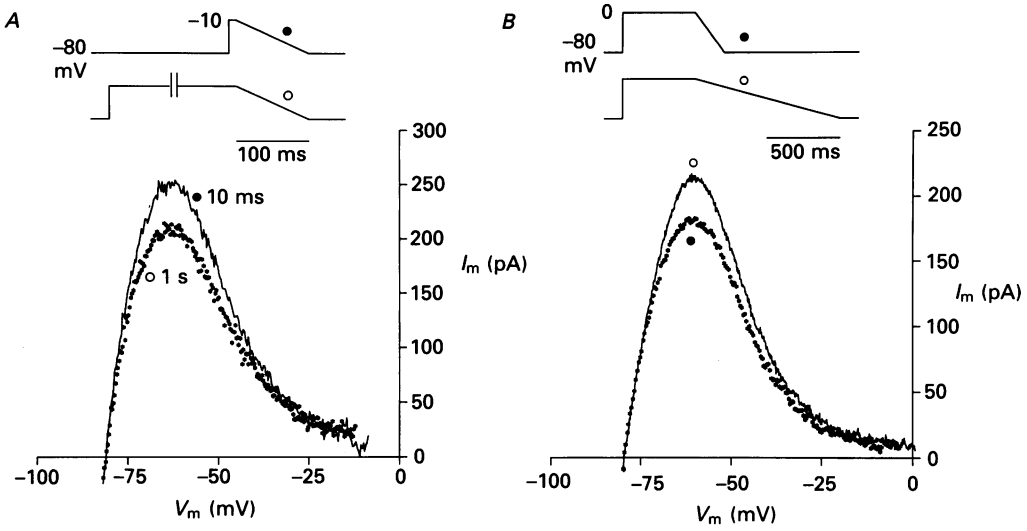

Fig. 11. *A*, effect of a 'conditioning' depolarization on I_{K1} generated during a linear potential ramp voltage-clamp protocol, shown schematically above. The ramp (from −10 to −80 mV, in 100 ms) was preceded either by a 1 s (○) or a 10 ms (●) 'conditioning' step to −10 mV. The current–voltage relations for I_{K1} during both ramps are superimposed. The peak magnitude of I_{K1} was larger for the ramp with the 10 ms 'conditioning'. *B*, effect of the rate of change of membrane potential on I_{K1} generated during ramp voltage-clamp protocols. The protocols are shown in the inset. The ramps (from 0 to −80 mV, in 0·2 s (●) or 1 s (○)) were preceded by a 500 ms 'conditioning' step at 0 mV. The current–voltage relations for I_{K1} from both ramps are superimposed. The peak magnitude of I_{K1} during the slower ramp (○) was larger than that during the faster ramp (●). Temperature was 32 °C.

DISCUSSION

Summary of results

The results presented here demonstrate that the inwardly rectifying potassium current, I_{K1}, in rabbit ventricular myocytes exhibits slow time- and voltage-dependent behaviour in a range of membrane potentials which corresponds to the plateau and repolarization phases of the action potential. As a consequence, I_{K1} is partially 'inactivated' during the plateau phase of the action potential, and the magnitude of I_{K1} during repolarization is less than that measured under conditions which are closer to a 'steady state' (e.g. Fig. 10). These relatively small current changes are functionally important since they result in alterations in the height of the plateau and duration of the action potential, and therefore can modulate both excitation–contraction coupling and refractoriness. Although current changes resulting from inactivation and reactivation of I_{K1} have been studied previously in egg cells (e.g. Ohmori 1978), frog muscle (e.g. Hestrin, 1981), neonatal heart (e.g. Josephson, 1988) and myocytes from adult guinea-pig and rabbit heart (Harvey & ten Eick, 1988, 1989*a*, *b*; Ishihara, Mitsuiye, Noma & Takano, 1989; Anumonwo,

Demar & Jalife, 1990), many of these recordings have been made in a range of potentials between −90 and −150 mV, and therefore are unlikely to be important in normal electrophysiological responses.

A number of our results suggest that the slow tail currents in step voltage-clamp protocols when the membrane was repolarized to potentials in the range −30 to −70 mV after a depolarization to plateau potentials (−10 to +10 mV), result from a time-dependent increase in the magnitude of I_{K1}: (i) the membrane potential and $[K^+]_o$ dependence of steady-state outward I_{K1} and tail current magnitudes were closely correlated; (ii) I_{K1} and tail currents were simultaneously abolished by external application of Ba^{2+} or removal of external K^+; (iii) Ba^{2+}- and K^+-sensitive tail currents were absent in rabbit atrial myocytes, which have very little I_{K1} (Giles & Imaizumi, 1988) and (iv) tail currents were present in ventricular cells in which changes in intracellular $[Ca^{2+}]$ were inhibited by internal EGTA or after blocking the voltage-dependent calcium current, thus distinguishing the tail currents from current transients associated with the Na^+–Ca^{2+} exchange process (Giles & Shimoni, 1989; Earm *et al.* 1990).

Limitations of the action potential voltage-clamp method

Convincing isolation of a specific component of membrane current using the AP voltage-clamp method requires that the current change of interest can be blocked both selectively and completely. In this study, I_{K1} was isolated from other membrane currents that were activated during the action potential by removing external K^+ and thereby abolishing I_{K1}. It was important to ensure that this procedure selectively abolished I_{K1}, because other K^+ currents, e.g. transient outward (I_t; Giles & Imaizumi, 1988) and delayed rectifier currents, are also changed significantly by removal of external K^+. 4-AP was routinely used to block I_t (Giles & Imaizumi, 1988). No attempt was made to block the delayed rectifier, but this current is very small in rabbit ventricular myocytes, especially at room temperatures (Giles & Imaizumi, 1988). Complete removal of external K^+ is known to block the Na^+–K^+ pump activity (Gadsby, 1984), and since this transport process is electrogenic, a current component due to the Na^+–K^+ pump could contaminate the measurements of I_{K1}. Hence, ouabain was included in the superfusing solutions in order to block Na^+–K^+ pump activity. Use of Ba^{2+} to block I_{K1} proved to be unsatisfactory, since it was apparent that at a concentration of 0·5 mM of Ba^{2+}, I_{K1} was 10–20% smaller during both AP voltage clamp and ramp protocols than values obtained by removal of external K^+ in the same cells. This difference possibly resulted from the voltage dependence of Ba^{2+} block of I_{K1} (Standen & Stanfield, 1978*b*; DiFrancesco, Ferroni & Visentin, 1984).

Time and voltage dependence of the inward rectifier

Recent work has given important new insights into the mechanisms underlying inward rectification in the heart (Oliva *et al.* 1990; Matsuda, 1991). These results suggest that there are two independent, voltage-dependent mechanisms which contribute to the reduction of outward current through the I_{K1} channels at membrane potentials positive to E_K. The first of these is voltage-dependent *closing* (due to deactivation) of the I_{K1} channels (Kurachi, 1985; Matsuda *et al.* 1987); the

second is voltage-dependent *block* of the channel by internal Mg^{2+} (Matsuda *et al.* 1987; Vandenburg, 1987; Matsuda, 1988, 1991) and Ca^{2+} ions (Mazzanti & DiFrancesco, 1989). These mechanisms combine to produce the strong inward rectification and negative slope characteristics of the steady-state I_{K1} current–voltage relationship (Ishihara *et al.* 1989; Oliva *et al.* 1990). The kinetics of both channel closing and Mg^{2+} block are very fast at membrane potentials positive to E_K, giving rise to 'quasi-instantaneous' current changes on depolarization. The step voltage-clamp protocols used in this study show that in addition to the very rapid processes, there is a 'slow' process which develops during membrane depolarization. This process 'inactivates' I_{K1}, and it is the removal of this 'inactivation' during repolarization to more negative potentials that results in the slow I_{K1} tail currents. Two aspects of this slow process should be noted. First, the onset of depolarization-induced 'inactivation' is slow and requires 100–300 ms to completely develop, as shown by the 'envelope-of-tails' protocol in Fig. 5. Second, the removal of 'inactivation' is equally slow, and is strongly voltage dependent between −40 and −70 mV (Fig. 7). If it is assumed that some removal of 'inactivation' occurs during a slow membrane potential change (e.g. action potential, or voltage ramp), the kinetics of I_{K1} recovery may explain why a more rapid rate of voltage change from positive to negative membrane potentials elicits less outward I_{K1} than does a slower rate (e.g. Figs 10 and 11).

The slow kinetic processes recorded using whole-cell voltage-clamp techniques cannot be studied at the single-channel level under physiological conditions, since outward currents through single I_{K1} channels are undetectable with 'normal' intracellular $[Mg^{2+}]$ (Matsuda *et al.* 1987; Vandenburg, 1987; but see Mazzanti & DeFelice, 1990). However, channel gating during outward current flow can be directly observed when $[Mg^{2+}]_i$ is reduced to micromolar levels. Matsuda (1988) has shown that I_{K1} channels can exhibit long-lived (tens to hundreds of millisecond) closed states during depolarizations positive to E_K, and it is possible that these long-lived states underlie the 'inactivation' of I_{K1} seen in whole-cell recordings. It is unclear whether or not the long-lived closed states result directly from Mg^{2+} ion block of the channel, or whether they are an intrinsic, voltage-dependent gating process.

Functional significance of heart-rate-dependent changes in I_{K1}

We have identified a novel time- and voltage-dependent change in an inwardly rectifying K^+ current, I_{K1}, in myocytes from rabbit ventricle. Although this current change is relatively small (10–30 pA), it may produce a significant voltage change in those phases of the cardiac action potential which are regulated by a very small net current, e.g. the plateau (Noble, 1984). In addition, the increase in outward current resulting from reactivation of I_{K1} following repolarization may be one of the factors regulating the threshold for action potential firing; thus it may modulate the refractory period, particularly when, for example the sodium current is decreased by a small (5–10 mV) depolarization of the resting potential.

This study was supported by the Canadian Medical Research Council (PG-44), the Heart and Stroke Foundation of Canada, and the Alberta Heritage Foundation for Medical Research (AHFMR). W. Giles is an AHFMR Medical Scientist.

REFERENCES

ADAMS, D. J. & NONNER, W. (1989). Voltage-dependent potassium channels: gating, ion permeation and block. In *Potassium Channels: Structure, Classification, Function and Therapeutic Potential*, ed. COOK, N. S., pp. 40–69. Ellis Harwood Ltd, Chichester.

ANUMONWO, J. M. B., DELMAR, M. & JALIFE, J. (1990). Electrophysiology of single heart cells from the rabbit tricuspid valve. *Journal of Physiology* **425**, 145–167.

BIERMANS, G., VEREECKE, J. & CARMELIET, E. (1987). The mechanism of the inactivation of the inward-rectifying K current during hyperpolarization steps in guinea-pig ventricular myocytes. *Pflügers Archiv* **410**, 604–613.

CARBONE, A. & LUX, H. D. (1987). Kinetics and selectivity of low-voltage-activated calcium current in chick and rat sensory neurones. *Journal of Physiology* **386**, 547–570.

CARMELIET, E. (1982). Induction and removal of inward-going rectification in sheep cardiac Purkinje fibres. *Journal of Physiology* **327**, 285–308.

DIFRANCESCO, D., FERRONI, A. & VISENTIN, S. (1984). Barium-induced blockade of the inward rectifier in calf Purkinje fibers. *Pflügers Archiv* **402**, 446–453.

DIFRANCESCO, D. & NOBLE, D. (1985). A model of cardiac electrical activity incorporating ionic pumps and concentration changes. *Philosophical Transactions of the Royal Society* B **307**, 353–398.

DOERR, T., DENGER, R., DOERR, A. & TRAUTWEIN, W. (1990). Ionic currents contributing to the action potential in single ventricular myocytes of the guinea pig studied with action potential clamp. *Pflügers Archiv* **416**, 230–237.

EARM, Y. E., HO, W. K. & SO, I. S. (1990). Inward current generated by Na–Ca exchange during the action potential in single atrial cells of the rabbit. *Proceedings of the Royal Society* B **240**, 61–81.

GADSBY, D. C. (1984). The Na/K pump of cardiac cells. *Annual Review of Biophysics and Bioengineering* **13**, 373–398.

GILES, W. R. & IMAIZUMI, Y. (1988). Comparison of potassium currents in rabbit atrial and ventricular cells. *Journal of Physiology* **405**, 123–145.

GILES, W. R. & SHIMONI, Y. (1989). Slow inward tail currents in rabbit cardiac cells. *Journal of Physiology* **417**, 447–463.

HAMILL, O. P., MARTY, A., NEHER, E., SAKMANN, B. & SIGWORTH, F. J. (1981). Improved patch-clamp techniques for high-resolution current recording from cells and cell-free membrane patches. *Pflügers Archiv* **391**, 85–100.

HARVEY, R. D. & TEN EICK, R. E. (1988). Characterization of the inward-rectifying potassium current in cat ventricular myocytes. *Journal of General Physiology* **91**, 593–615.

HARVEY, R. D. & TEN EICK, R. E. (1989*a*). On the role of sodium ions in the regulation of the inward-rectifying potassium conductance in cat ventricular myocytes. *Journal of General Physiology* **94**, 329–348.

HARVEY, R. D. & TEN EICK, R. E. (1989*b*). Voltage-dependent block of cardiac inward-rectifying potassium current by monovalent cations. *Journal of General Physiology* **94**, 349–361.

HESTRIN, S. (1981). The interaction of potassium with the activation of anomalous rectification in frog muscle membrane *Journal of Physiology* **317**, 497–508.

HILLE, B. & SCHWARZ, W. (1978). Potassium channels as multi-ion single-file pores. *Journal of General Physiology* **72**, 409–442.

HUME, J. R. & UEHARA, A. (1985). Ionic basis of different action potential configurations of single guinea-pig atrial and ventricular myocytes. *Journal of Physiology* **368**, 525–544.

HUTTER, O. F. & NOBLE, D. (1960). Rectifying properties of heart muscle. *Nature* **188**, 495.

ISHIHARA, K., MITSUIYE, T., NOMA, A. & TAKANO, M. (1989). The Mg^{2+} block and intrinsic gating underlying inward rectification of the K^+ current in guinea-pig cardiac myocytes. *Journal of Physiology* **419**, 297–320.

JOSEPHSON, I. R. (1988). Properties of inwardly rectifying K^+ channels in ventricular myocytes. *Molecular and Cellular Biochemistry* **80**, 21–26.

KURACHI, Y. (1985). Voltage-dependent activation of the inward-rectifier potassium channel in the ventricular cell membrane of guinea-pig heart. *Journal of Physiology* **366**, 365–385.

MATSUDA, H. (1988). Open-state substructure of inwardly rectifying potassium channels revealed by magnesium block in guinea-pig heart cells. *Journal of Physiology* **397**, 237–258.

MATSUDA, H. (1991). Magnesium gating of the inwardly rectifying K^+ channel. *Annual Review of Physiology* **53**, 289–298.

MATSUDA, H., SAIGUSA, A. & IRISAWA, H. (1987). Ohmic conductance through the inwardly rectifying K^+ channel and blocking by internal Mg^{2+}. *Nature* **325**, 156–159.

MAZZANTI, M. & DEFELICE, L. J. (1990). Ca modulates outward current through I_{K1} channels. *Journal of Membrane Biology* **116**, 41–45.

MAZZANTI, M. & DIFRANCESCO, D. (1989). Intracellular Ca modulates K-inward rectification in cardiac myocytes. *Pflügers Archiv* **413**, 322–324.

NOBLE, D. (1965). Electrical properties of cardiac muscle attributable to inward going (anomalous) rectification. *Journal of Cellular and Comparative Physiology* **66**, 127–136.

NOBLE, D. (1984). The surprising heart: a review of recent progress in cardiac electrophysiology. *Journal of Physiology* **353**, 1–50.

OHMORI, H. (1978). Inactivation kinetics and steady-state noise in the anomalous rectifier of tunicate egg cell membranes. *Journal of Physiology* **281**, 77–99.

OLIVA, C., COHEN, I. S. & PENNEFATHER, P. (1990). The mechanism of rectification of i_{K1} in canine Purkinje myocytes. *Journal of General Physiology* **96**, 299–319.

ROBINSON, K. & GILES, W. (1986). Menu-driven A/D conversion, display and plotting programs for the IBM PC in electrophysiological studies. *Computer Methods and Programs in Biomedicine* **23**, 319–329.

RUDY, B. (1988). Diversity and ubiquity of K channels. *Neuroscience* **25**, 729–749.

SAKMANN, B. & TRUBE, G. (1984*a*). Conductance properties of single inwardly rectifying potassium channels in ventricular cells from guinea-pig heart. *Journal of Physiology* **347**, 641–657.

SAKMANN, B. & TRUBE, G. (1984*b*). Voltage-dependent inactivation of inward-rectifying single-channel currents in the guinea-pig cell membrane. *Journal of Physiology* **347**, 659–683.

STANDEN, N. B. & STANFIELD, P. R. (1978*a*). Inward rectification in skeletal muscle: a blocking particle model. *Pflügers Archiv* **378**, 173–176.

STANDEN, N. B. & STANFIELD, P. R. (1978*b*). Potential and time dependent blockade of inward rectification in frog skeletal muscle fibre by barium and strontium ions. *Journal of Physiology* **280**, 169–191.

TOYOTOMI, S. & MOMOSE, Y. (1989). Temperature-controlled perfusion apparatus for microscope using transparent conducting film heater. *American Journal of Physiology* **256**, C214–217.

TSENG, G. N., ROBINSON, R. B. & HOFFMAN, B. F. (1987). Passive properties and membrane currents of canine ventricular myocytes. *Journal of General Physiology* **90**, 671–701.

VANDENBERG, C. A. (1987). Inward rectification of a potassium channel in cardiac ventricular cells depends on internal magnesium ions. *Proceedings of the National Academy of Sciences of the USA* **84**, 2560–2564.